applied sciences

MDPI

Article

Visible—Light Driven Systems: Effect of the Parameters Affecting Hydrogen Production through Photoreforming of Organics in Presence of Cu_2O/TiO_2 Nanocomposite Photocatalyst

Marica Muscetta [1,*], Laura Clarizia [1,*], Marco Race [2], Roberto Andreozzi [1], Raffaele Marotta [1] and Ilaria Di Somma [3]

[1] Department of Chemical Engineering, Materials and Industrial Production, University of Naples Federico II, Corso Umberto I, 40, 80138 Napoli, Italy
[2] Department of Civil and Mechanical Engineering, University of Cassino and Southern Lazio, Via di Biasio 43, 03043 Cassino, Italy
[3] Istituto di Scienze e Tecnologie per l'Energia e la Mobilità Sostenibili (CNR), 80125 Naples, Italy
* Correspondence: marica.muscetta@unina.it (M.M.); laura.clarizia2@unina.it (L.C.)

Abstract: Several studies have shown that combining TiO_2 and Cu_2O enhances the photocatalytic activity of the material by generating a heterojunction capable of extending the light absorption in the visible and reducing the electron-hole recombination rate. Ball milling has been chosen as an alternative methodology for photocatalyst preparation, among the several techniques documented in the literature review. The results of a previously reported investigation enabled the identification of the most effective photocatalyst that can be prepared for hydrogen generation by combining Cu_2O and TiO_2 (i.e., 1%wt. Cu_2O in TiO_2 photocatalyst prepared by ball-milling method at 200 rpm and 1 min milling time). To optimize photocatalytic hydrogen generation in the presence of the greatest photocatalyst, the effects of (i) sacrificial species and their concentration, (ii) temperature, and (iii) pH of the system are taken into account, resulting in a light-to-chemical energy efficiency of 8% under the best-tested conditions. Last but not least, the possibility of using the present photocatalytic system under direct solar light irradiation is evaluated: the results indicate that nearly 60% of the hydrogen production recorded under sunlight can be attributed to the visible component of the solar spectrum, while the remaining 40% can be attributed to the UV component.

Keywords: green hydrogen; photoreforming; ball milling; cuprous oxide; solar photocatalysis

check for updates

Citation: Muscetta, M.; Clarizia, L.; Race, M.; Andreozzi, R.; Marotta, R.; Di Somma, I. Visible—Light Driven Systems: Effect of the Parameters Affecting Hydrogen Production through Photoreforming of Organics in Presence of Cu_2O/TiO_2 Nanocomposite Photocatalyst. *Appl. Sci.* **2023**, *13*, 2337. https://doi.org/10.3390/app13042337

Academic Editor: Michalis Konsolakis

Received: 29 January 2023
Revised: 6 February 2023
Accepted: 8 February 2023
Published: 11 February 2023

Copyright: © 2023 by the authors. Licensee MDPI, Basel, Switzerland. This article is an open access article distributed under the terms and conditions of the Creative Commons Attribution (CC BY) license (https://creativecommons.org/licenses/by/4.0/).

1. Introduction

Due to global environmental difficulties and the depletion of fossil resources, sustainable energy generation is one of the most important tasks of this century [1]. Hydrogen is a viable alternative energy carrier because of its stability, abundance on Earth's surface, and lack of greenhouse gas emissions [2–7]. Due to its renewability, the use of solar energy to make hydrogen is an appropriate technique for meeting the energy demand [4,8–13]. Photo reforming of organics in the aqueous phase [14–16] is an emerging technique able to combine wastewater treatment and energy production. The creation of visible—light active and stable photocatalytic/photo electrocatalytic materials is now the greatest obstacle for many researchers, despite a large number of photocatalysts suggested for hydrogen production [17]. Despite TiO_2 still representing the most used material, due to its advantages (chemical stability, photo corrosion resistance, non-toxicity, widespread availability, etc.), it presents various problems such as a high electron–hole recombination rate (3.0×10^{10} M^{-1} s^{-1} [18]) and poor absorption in the visible light range, due to its wide band gap (about 3.2 eV) [19]. To overcome these disadvantages, many researchers have directed their efforts to improve the efficiency of bare TiO_2 through the combination of the semiconductor with other materials capable to extend the light absorption to the visible

range and/or to reduce the recombination rate [8,20]; on the other hand, many studies present in the literature are focused on the utilization of different semiconductors able to replace TiO_2 [21–23].

With reference to the first approach, noble metals (Ag, Pt, Au, Pd) have been found to be excellent co–catalysts for hydrogen production [24,25], despite the fact that they have high costs; impregnation, co-precipitation or photodeposition methods are only some examples of the preparation methods proposed for metal-doped photocatalyst by several authors [26,27].

Generally, noble metals have gained great attention due to their physicochemical characteristics, which effectively enhance the photocatalytic activity; in particular, the deposition of metals with a large work function, such as Ag, Au as well as Pt and Pd can reduce the recombination rate because of the formation of Schottky barriers at the metal/TiO_2 interface: being the work function of the metal higher than that of the titanium dioxide there is the formation of an electrons flow from TiO_2 to the metal to align the Fermi energy levels (EF), with a shift of the Fermi levels of the metal to the conduction band of TiO_2 [28]. The metal, with more negative energy levels, leads to a thermodynamically favourable proton ion reduction and favours the proton reduction also from a kinetic point of view. Hence, metal nanoparticles (a) act as antennas, producing a higher light absorption and (b) promote the transfer of free excited electrons into the conduction band of the semiconductor [29]. Despite the improvement in the photocatalytic activity of the metal–doped photocatalysts, these materials do not demonstrate a significant activation under visible light radiation. Hence, to extend the light adsorption to a wavelength higher than 400 nm, a different approach was proposed by some authors: among the techniques to improve the photocatalytic activity of the photocatalysts, many researchers have proposed the combination of semiconductors, such as TiO_2, with other materials capable of extending the visible light absorption to the visible range [8,20,30,31]. The association of two (or more) different semiconductors (semiconductor–semiconductor heterojunction) was discussed in several articles [32–37]. Generally, two different categories of semiconductor–semiconductor photocatalytic materials are reported: p–n semiconductor heterojunction and non–p–n heterojunction systems. Focusing the attention on the first case, when two semiconductors (a p–type semiconductor with a n–type semiconductor) are in contact, the diffusion of electrons and holes leads to the formation of a space–charge region at the interfaces. When irradiated, the photogenerated electrons are transferred from the CB of one photocatalyst (generally the p–type) to the CB of the other photocatalyst forming the heterojunction (generally the n–type), while the holes can migrate between the valence bands of the semiconductors, depending on the relative redox potentials; the phenomenon leads to more efficient charge separation and a lower electron-holes recombination rate. The heterojunction formation by combining TiO_2 (n–type semiconductor) and Cu_2O (p–type semiconductor) is a viable route to improve solar light utilization [38–41]. Among the different techniques reported in the literature to prepare Cu_2O/TiO_2 composite material, a simple and industrially practicable ball milling procedure to dryness was selected as an alternate strategy for preparing photocatalysts in our recent study [42]. The results of the previous study allowed the selection of the best photocatalyst for hydrogen generation prepared by mixing Cu_2O and TiO_2 (i.e., 1%wt. Cu_2O in TiO_2 photocatalyst material prepared through ball milling method at a rotation rate of 200 rpm and milling time of 1 min). In the present work, we have chosen to use the best photocatalyst identified previously, to evaluate the possibility to use real solar conditions to produce hydrogen. Firstly, to optimize the photocatalytic hydrogen production in presence of the best-performing photocatalyst, the effect of the following variables on the hydrogen production is herein investigated:

The concentration of the sacrificial species;
Type of sacrificial species used;
Temperature and pH of the system;
Then, the photoefficiency under direct sunlight irradiation was evaluated.

The quantum yield and the light-to-chemical energy are estimated under the optimal conditions seen based on the data.

2. Materials and Methods

2.1. Materials

TiO_2 nanopowder (commercial grade, Aeroxide TiO_2-P25, average particle size 21 nm, specific surface area 50 ± 15 $m^2 \cdot g^{-1}$, 80/20 anatase/rutile), ethanol (absolute, ≥99.8%), glycerol (ACS reagent, ≥99.5%), formic acid (puriss. p.a., ACS reagent, ≥98%), lactic acid (85%, FCC), ethylene glycol (anhydrous, 99.8%) were purchased from Sigma Aldrich (Pty Ltd.), while cuprous oxide (Cu_2O, powder) and methanol (99.9%) are purchased from Carlo Erba Reagents (Cornaredo, MI). All reagents are used as received. Doubly glass–distilled water is used.

2.2. Preparation of the Photocatalyst

The synthesis of the photocatalyst is performed by following the procedure reported by Muscetta et al. [42], in which the catalyst is characterized in detail. In particular, a fixed amount of TiO_2 (1500 mg) is mixed in the agate milling tank (PM100, RETSCH), with agate balls and a fixed amount of Cu_2O (150 mg), fixing the rotation rate to 200 rpm and the milling time to 1 min. In the following sections, the photocatalytic material used, with a surface area of 57.5 m^2/g, will be named (1%wt.) Cu_2O/TiO_2.

2.3. Photocatalytic Tests and Analytical Determination

Photocatalytic tests are performed as in [42] (see Figure 1A,B for the schematic illustration of the experimental setup). A UV cutoff solution ($NaNO_2$ 0.5 M) is pumped through the quartz sleeve to allow the investigation of the photocatalytic activity under visible light conditions (λ > 400 nm), as reported by others [43]. To perform a typical experimental run, 210 mg of Cu_2O-TiO_2 catalyst are suspended in a doubly distilled aqueous solution (V = 0.3 L), at fixed pH and concentration of the sacrificial species. In particular, to evaluate the effect of the sacrificial species on the photocatalytic activity, a fixed concentration (2.5 M) of each scavenger (i.e., methanol, ethanol, ethylene glycol, formic acid, glycerol, lactic acid) was used. The effect of the organic concentration was assessed by fixing methanol concentration between 0 and 2.5 M. A N_2 stream is bubbled into the solution starting 40 min before inserting the photocatalyst to prevent the interaction between dissolved oxygen and copper species or photogenerated electrons. The effect of the temperature was assessed by increasing the temperature of the system up to 80 °C (at this temperature a condenser was located on the reactor to prevent the evaporation of the organic species). To test the effect of pH, in some runs the solution pH is corrected to selected values by adding a diluted solution of KOH or $HClO_4$.

The suspension, containing a fixed concentration of the sacrificial agent (2.5 M) and a fixed amount of the photocatalytic material (700 ppm), was exposed to solar radiation (See the Figure 1B for the schematic illustration of the experimental set–up) to evaluate the photoefficiency of the system under solar light irradiation in selected runs. These runs were carried out in early September 2021 in Naples (40°50′0″ N, 14°15 0″ E), between the hours 11.00 and 13.00 under clear sky conditions. To evaluate the separate contribution of the UV and visible radiation ranges in hydrogen production, some photocatalytic runs are carried out by employing a cut-off filter to eliminate radiations with wavelengths less than 400 nm. In some cases, the recovery of the material was performed following the procedure reported previously [42].

Hydrogen estimation is carried out as reported elsewhere [42,44]. The pH of the solution is measured using an Orion 420 p pH–meter (Thermo). Shimadzu UV-2600 UV/vis spectrophotometer was used for UV-vis diffusive reflectance analysis, with an integrating sphere attachment and $BaSO_4$ as the reflectance standard. A Quantachrome Autosorb 1-C instrument analyzer was employed to evaluate the textural properties of catalysts [42].

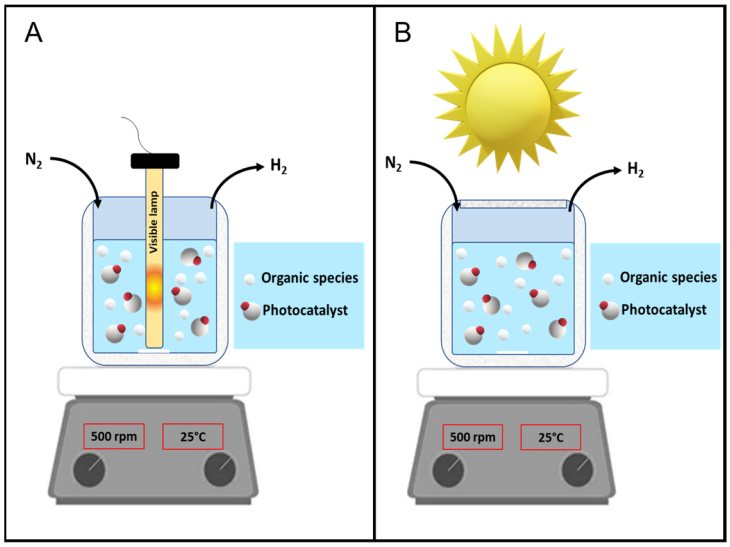

Figure 1. Schematic illustration of the annular batch reactor experimental set-up for the experiments conducted (**A**) under artificial UV and/or Visible light source and (**B**) under solar irradiation.

3. Results and Discussion

3.1. Effect of Organic Concentration

The effect of the different parameters affecting the preparation stage of the photocatalyst in the presence of methanol was previously discussed [42]. The influence of methanol concentration on the photocatalytic generation of hydrogen is herein explored. The main results are reported in Figure 2. The reaction rate observed during the photocatalytic runs at varying organic concentrations is properly described by a Langmuir–Hinshelwood model. The adsorbed species concentration may be thus calculated through the equilibrium reaction (1) and the Equation (1), in which K_{ads} (M^{-1}) is the adsorption equilibrium constant and θ_{free} is the concentration of free active sites on the catalyst surface:

$$CH_3OH + \theta_{free} \overset{K_{ads}}{\leftrightarrow} CH_3OH_{ads} \quad \text{(R1)}$$

$$K_{ads} = \frac{[CH_3OH_{ads}]}{\theta_{free}[CH_3OH]} \quad (1)$$

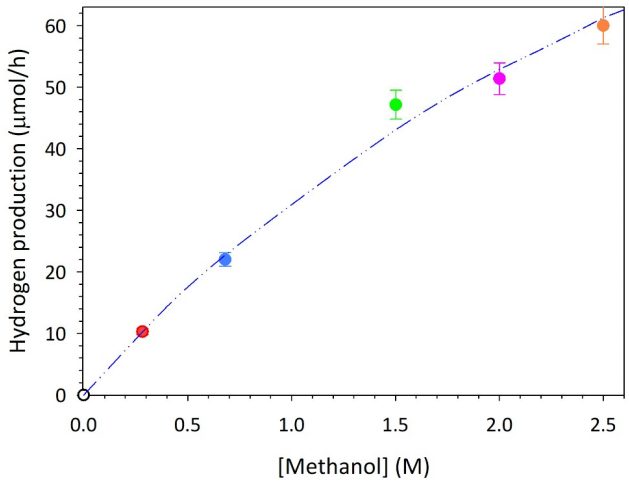

Figure 2. Hydrogen evolution rate at different organic concentrations (methanol). Experimental conditions: V = 0.30 L; T = 35 °C; P = 1 atm; pH ≈ 8.5; $C_{(1\%wt.)Cu_2O/TiO_2}$ = 700 ppm.

To obtain a value of the adsorption constant (K_{ads}) for methanol over the Cu_2O/TiO_2 composite photocatalyst, the following Langmuir–Hinshelwood–type model describing hydrogen generation rate is adopted (2):

$$r_{H_2} = k'' \frac{K_{ads}[CH_3OH]}{1 + K_{ads}[CH_3OH]} \quad (2)$$

where $k'' = k' \cdot \theta_t$ (k' being the kinetic constant) and K_{ads} are the apparent kinetic constant of substrate oxidation and the organic adsorption constant, respectively. θ_t (M) is the concentration of the total active site on the catalyst surface for a fixed catalyst load q(g/L). The term θ_t is calculated through the following Equation (3):

$$\theta_t = N \cdot q \quad (3)$$

where N is the total moles of active sites per unit mass of catalyst (mol/g).

Starting from Equation (3) and plotting the reciprocal of the hydrogen reaction rate versus the reciprocal of the organic concentration (Figure 3), a linear trend is observed, from which a suitable value for K_{ads} is obtained. By following the optimization procedure reported elsewhere [44], a value of 0.22 M^{-1} is found in presence of the photocatalyst tested when methanol is used as a scavenger. This value resulted in accordance with those reported in the literature for similar systems in presence of the same organic compound [45].

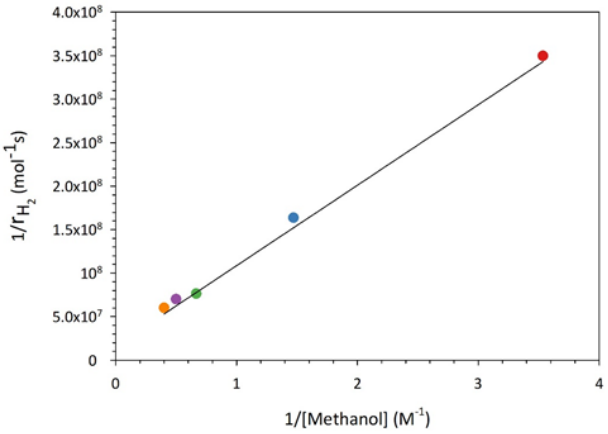

Figure 3. Reciprocal of the hydrogen production vs. the inversus of the organic concentration. Experimental conditions: V = 0.30 L; T = 35 °C; P = 1 atm; pH ≈ 8.5; $C_{(1\%wt.)Cu_2O/TiO_2}$ = 700 ppm.

3.2. Effect of pH

Some authors have reported a considerable effect of the suspension pH on the photocatalytic hydrogen generation for different photocatalytic materials and scavengers [41,44,46–48]. To evaluate the effect of this variable on the photoactivity, several runs are carried out at varying the solution pH. Figure 4 reports the mean hydrogen production rate collected at different pH values. A higher reactivity may be recognized under alkaline conditions, whereas negligible activity is recorded at acidic conditions (data not shown). Despite the great number of studies in the literature survey focusing on the effect of pH, only a few authors have attempted to explain the correlation between solution pH and photocatalytic activity [44,49–51]. The surface properties of the photocatalyst, its stability in the aqueous solution, the band gap shift, and the sacrificial agent's molecular properties should be considered to understand the phenomenon.

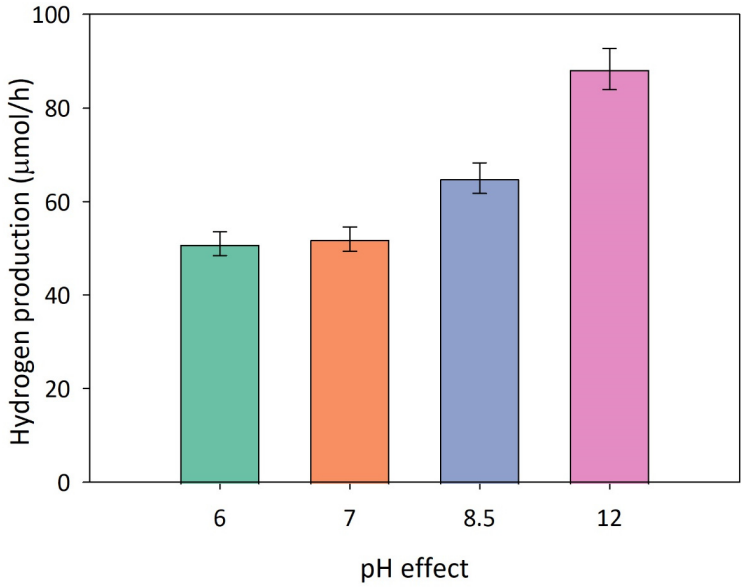

Figure 4. Hydrogen evolution rate at varying the pH of the suspension. Experimental conditions: V = 0.30 L; P = 1 atm; T = 35 °C; [Methanol] = 2.5 M; $C_{(1\%wt.)Cu_2O/TiO_2}$ = 700 ppm; visible range.

The following remarks should be considered to underpin the present photocatalytic outcomes:

- The stability of the copper species on the surface of TiO_2 particles is affected by the pH. In particular, lower stability is recorded by several authors under acidic conditions [49,52,53].
- About Methanol (i.e., the sacrificial agent), has a pK_a value of 15.0 [54]. Thus, methanol is present in non-dissociated form for all the pH values tested (See Figure 5).
- The pH_{zpc} of TiO_2 is about 6.25 [55]. Thus, a high concentration of negative charges is recorded on the catalyst surface under alkaline conditions (See Figure 5), able to promote the interaction between substrate and catalyst surface.
- Negative charges on the catalyst surface (under alkaline conditions) reduce particle agglomeration [56].

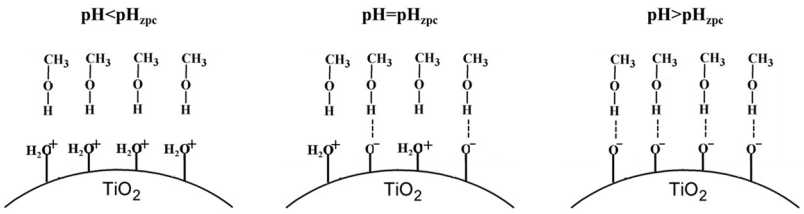

Figure 5. Schematic illustration of adsorption conditions of methanol on the photocatalytic Titania surface at different pH values.

Based on the above considerations, the greater photocatalytic activity under alkaline conditions may be attributed to (i) the presence of stable copper species involved in visible light-induced hydrogen generation and (ii) the more efficient adsorption of the organic compounds.

3.3. Effect of Temperature

Photocatalytic processes are generally reported to be poorly influenced by the temperature, as the electron-hole generation mainly depends on the radiation intensity [57]. However, the temperature may improve the activity of the system, being able to (i) increase the reaction rate of the hydrogen generation and (ii) improve the product desorption from the catalyst [58]. As a result, according to different authors [59–61], temperature helps the

hydrogen generation reaction compete more successfully with charge-carrying recombination. For this reason, some experimental runs are performed varying the temperature of the suspension between 20 °C and 80 °C, in presence of methanol as a scavenger. The main results are reported in Figure 6. As clearly sown by the diagram, when the temperature increases from 20 °C to 80 °C, the hydrogen production rate achieves a value about 4.5 times higher than that obtained at the lowest temperature, thus proving the beneficial effect of temperature on the system behaviour.

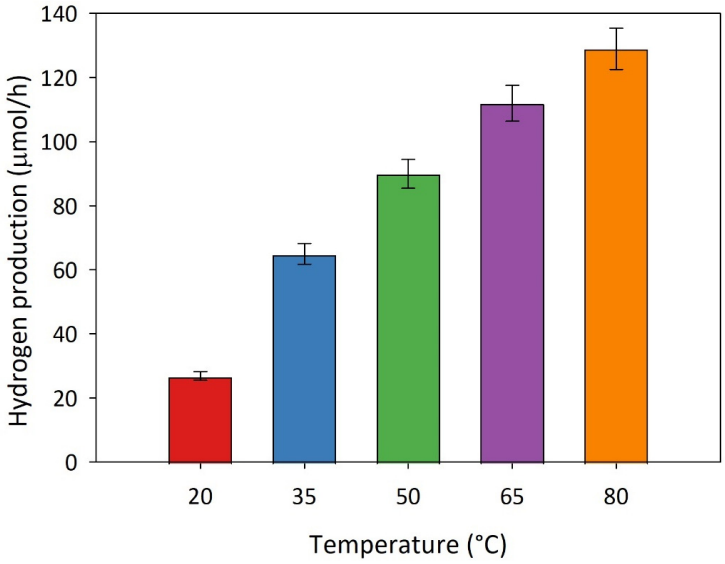

Figure 6. Hydrogen evolution rate at varying the temperature of the system. Experimental conditions: V = 0.30 L; P = 1 atm; pH ≈ 8.5; [Methanol] = 2.5 M; $C_{(1\%wt.)Cu_2O/TiO_2}$ = 700 ppm; visible range.

By considering that the photocatalytic hydrogen production follows a pseudo-first-order law for all the temperatures tested, it is possible to plot the Arrhenius-type equation from 293 K to 353 K (See Figure 7). A value of 21.51 KJ/mol is easily estimated for the apparent activation energy E_a from the slope of the Arrhenius plot. Such a value is consistent with those reported in the literature survey for similar systems [61,62].

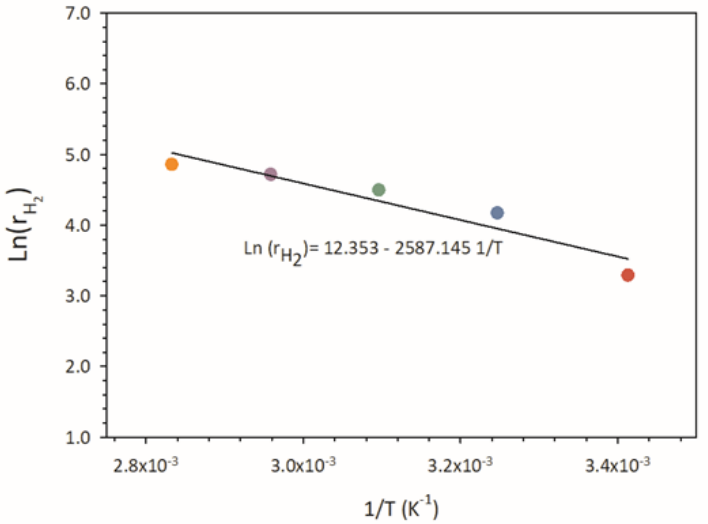

Figure 7. Arrhenius plot for (1%wt.) Cu_2O/TiO_2 photocatalyst.

3.4. Effect of the Sacrificial Agent

Many researchers proposed hydrogen production through photoreforming of organics in the aqueous phase [14–16]. Organic species may derive from renewable sources or

organic-rich effluents [63–65]. Due to (i) the possibility of linking hydrogen generation with water treatment and (ii) the cheap cost of the feedstock, the potential use of organic contaminants found in wastewater is particularly appealing [63,66–68]. Evaluating the effect of the scavenger used on photocatalytic hydrogen production is thus necessary. To this aim, some experimental runs are carried out at varying the sacrificial species (i.e., alcohols or carboxylic acids). The main results collected during this investigation are reported in Figure 8. Glycerol and 1,2–Ethandiol result in the greatest options for hydrogen generation in presence of Cu_2O/TiO_2 photocatalyst, according to literature findings in which Cu-based TiO_2 was used to generate hydrogen through photoreforming [52]. On the contrary, no hydrogen production is herein detected in the case of pure water and seawater. Both the nucleophilicity of the groups in the molecular structure of the sacrificial agents and the capacity of the organics to adsorb on the catalyst surface affect the reactivity of the organics with photogenerated holes and can be used to explain these findings. The four species exhibiting the higher photoefficiency for hydrogen evolution (i.e., methanol, ethanol, glycerol and 1,2-ethanediol) have similar nucleophilicity values, as reported in Table 1. As regards the adsorption phenomenon, the development of the bidentate (and tridentate) complexes can be proposed for glycerol and 1,2-ethanediol. On the other hand, the creation of weaker monodentate complexes can be supposed for ethanol and methanol, according to their structures.

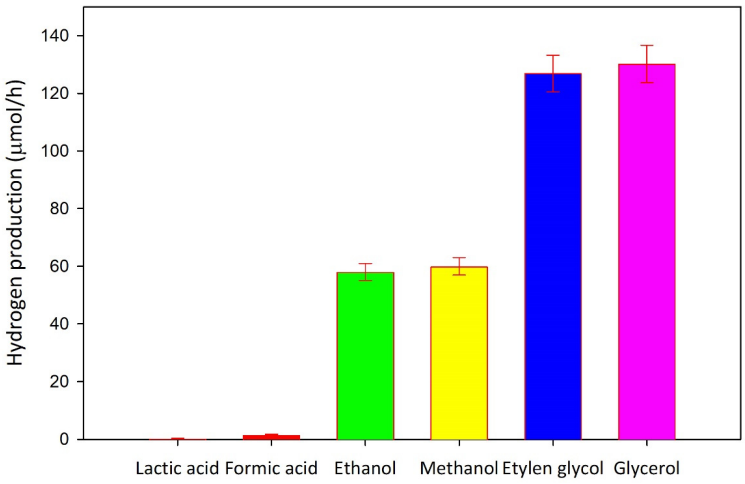

Figure 8. Hydrogen evolution in the presence of various organic species. Experimental conditions: V = 0.30 L; P = 1 atm; T= 35 °C; [Organic] = 2.5 M; $C_{(1\%wt.)Cu_2O/TiO_2}$ = 700 ppm; visible light radiation.

Table 1. pKa values of several compounds used in the experiments.

Organic Species	pKa Value	Natural pH of the Solution	Reference
Ethanol	15.9	7.0	[69]
Methanol	15.3	8.5	[54]
1,2-ethanediol	15.1	6.0	[54]
Glycerol	14.4	6.5	[54]
Lactic acid	3.86	2.0	[70]
Formic acid	3.75	3.0	[69]

By contrast, the almost negligible photo efficiency for hydrogen evolution recorded in the presence of formic acid and lactic acid can be related to the following phenomena: (i) acidic conditions (See Table 1) reduce the stability of copper species, as previously discussed; (ii) under acidic conditions, the photocatalyst surface is positively charged, thus exhibiting a weak interaction with the organic compounds. Based on these considerations, glycerol is the best sacrificial agent tested in this study. In addition, a beneficial effect of the

temperature on hydrogen evolution is observed also in the case of glycerol. Indeed, when glycerol is used as a scavenger and the system temperature of the system is set at 80 °C, the hydrogen generation rate achieves a value of 260 μmol·h^{-1}.

3.5. Efficiency Calculation

To easily compare the present photocatalytic outcomes with previous findings in the literature survey, the apparent quantum efficiency (AQE) and the light–to–chemical energy efficiency (η) are determined from the best photocatalytic data obtained according to the following Equations (4) and (5):

$$\text{AQE } (\%) = \frac{2 \cdot r_{H_2}}{\text{moles of incident photons/time}} \cdot 100 \quad (4)$$

$$\eta = \frac{r_{H_2} \left(- \Delta H^0_{comb} \right)}{I \cdot S} \quad (5)$$

where:

r_{H_2} (mol·s^{-1}) is the hydrogen generation rate;

ΔH^0_{comb} is the standard change in enthalpy for the combustion of hydrogen and oxygen ($-282.0 \cdot 103$ J · mol^{-1});

I (W · cm^{-2}) is the light source's specific irradiance;

S (cm^2) is the illuminated area.

In Figure 9 the most significant outcomes are reported. When a high–pressure Hg lamp is used, along with a (1% wt.) Cu_2O/TiO_2 composite photocatalyst prepared through the ball milling method (200 rpm, 1 min), at a system temperature of 80 °C, maximum AQE values of 3.17% and 6.54% are calculated under visible light radiation in presence of methanol and glycerol, respectively. Under identical circumstances, the maximum light–to–chemical energy efficiencies values of 1.16% and 2.36% are obtained for methanol and glycerol, respectively.

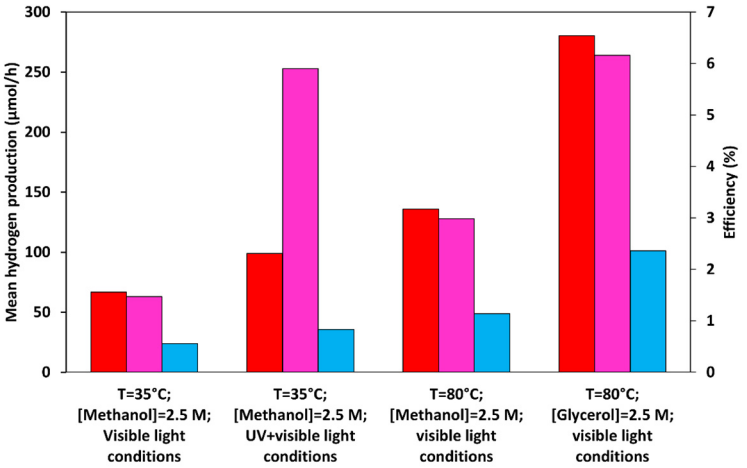

Figure 9. Mean hydrogen generation rate (■), AQE (■), and η (■) obtained under visible light irradiation (λ > 400 nm) and UV-A + Visible light conditions.

Additionally, the efficiency values obtained in the visible light spectrum (AQE = 1.56%, η = 0.56) are only slightly lower than those collected under identical circumstances (T = 35 °C, methanol as a scavenger) by using UVA + Visible light radiation (AQE = 2.31%, η = 0.83). In fact, as reported in the figure, despite the huge discrepancy in hydrogen generation in the presence and absence of UVA radiation, the different light intensities induce comparable activities in terms of quantum yield and light–to–chemical energy efficiency.

3.6. Photocatalytic Activity under Solar Conditions

To conclude the experimental campaign of the present study, a set of experiments are performed under direct solar irradiation by using the apparatus schematically represented in the Material and methods section (Figure 1B). Figure 10 reports the main results from the photocatalytic runs conducted under direct solar irradiation.

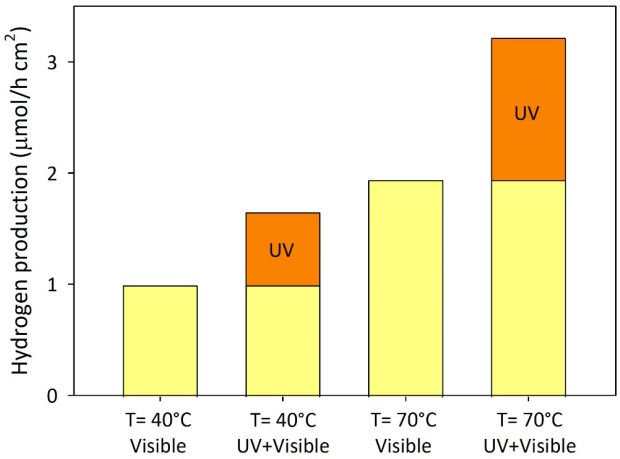

Figure 10. Hydrogen production rate during experimental runs conducted under direct sunlight irradiation. Experimental conditions: V = 0.30 L; P = 1 atm; pH ≈ 8.5; [MeOH] = 2.5 M; $C_{(1\%wt.)Cu_2O/TiO_2}$ = 700 ppm.

The hydrogen production rate is about 1 µmol·h^{-1}·cm^{-2} at the temperature of 40 °C and in the presence of visible light irradiation only. Hydrogen generation increases by about 1.6 times when all wavelengths of the solar spectrum are used. The result indicates that the contribution of the visible light portion of the solar spectrum supports about 60% of hydrogen production under sunlight radiation, whereas the improvement in hydrogen generation obtained without any UV cut-off filter may be ascribed to the UV component. Furthermore, as the temperature rises to 70 °C, the hydrogen generation rate increases to around 3 µmol·h^{-1}·cm^{-2}, demonstrating the favourable influence of temperature on photocatalytic activity. The efficiencies of the catalytic system adopted in the present investigation for hydrogen generation are calculated by using the irradiance values data collected during the experimental runs. The ranges of irradiation considered are 315–400 nm and 380–550 nm, where the mean values of the specific irradiances are about 15.56 W·m^{-2} and 95.75 W·m^{-2}, respectively. Table 2 reports the values of the light to chemical energy efficiency. A value of about 6.5% is obtained considering the contribution of the UV range at a system temperature of 70°C. As regards the light-to-chemical energy efficiency in the solar range, the low calculated values may result from an overestimation of the specific irradiance collected under the visible range (380–550 nm). Indeed, wavelengths higher than about 400 nm are completely useless for the activation of the adopted photocatalyst due to its bandgap value (i.e., 3.1 eV).

Table 2. Mean hydrogen production rate and light-to-chemical energy efficiency (in the UV and the visible range) obtained using the milled catalyst ($C_{(1\%wt.)Cu_2O/TiO_2}$) under direct sunlight irradiation.

Experimental Conditions	η (%) in the UV Range	η (%) in the Solar Range Explored
T = 40 °C; P = 1 atm; pH ≈ 8.5; C (1% wt.)Cu_2O/TiO_2 = 700 ppm; [Methanol] = 2.5 M; Solar light	3.33	1.16
T = 70 °C; P= 1 atm; pH ≈ 8.5; C(1% wt.) Cu_2O/TiO_2 = 700 ppm; [Methanol] = 2.5 M; Solar light	6.47	2.22

3.7. Activity under the Best Conditions

Eventually, the light-to-chemical energy efficiency is also estimated under the best conditions recorded in the previous sections. In particular, some photocatalytic experiments are carried out under direct sunlight radiation by fixing (i) the temperature of the system at 80 °C, (ii) the pH of the suspension at 12.0, and (iii) glycerol as a scavenger. Under these conditions, η reached a value of 8.15% in the UV range, and 2.81% in the visible light range only. Finally, the possibility of recycling the proposed material was investigated, observing a reduction in hydrogen production of about 40%, probably due to partial oxidation of copper (I), as well as some species not fully eliminated during the recovery of the material after the reaction.

4. Proposed Mechanism under Solar Radiation

An attempt to explain the mechanism of hydrogen generation is herein proposed and discussed (See Figure 11). As previously reported, cuprous oxide in the p–n heterojunction systems based Cu_2O/TiO_2 photocatalysts acts as an energy antenna [41], being able to absorb energy within the visible spectrum. Under direct sunlight radiation, in which the UV and the visible components are present, the activation of both semiconductors (i.e., Cu_2O and TiO_2) can be considered (See the reactions (2) and (3)):

$$Cu_2O \overset{h\nu}{\rightarrow} Cu_2O(h^+) + Cu_2O(e^-) \quad \text{(R2)}$$

$$TiO_2 \overset{h\nu}{\rightarrow} TiO_2(h^+) + TiO_2(e^-) \quad \text{(R3)}$$

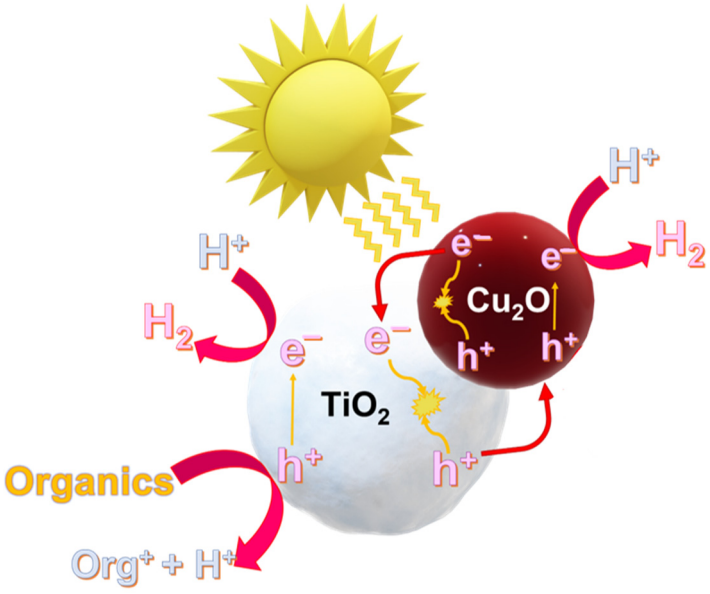

Figure 11. Schematic illustration of the proposed mechanism for hydrogen generation under solar light radiation in presence of Cu_2O/TiO_2 composite material.

After charge carrier generation, an electric field from TiO_2 to Cu_2O and band bending are established. Positive holes can react with the adsorbed organic species (mainly on the titania surface), following the reactions (4) and (5), thus forming byproducts and protons, which in turn can react with the photogenerated electrons to form $H_{2(g)}$ (through the reaction (6)).

$$Org + \theta_{TiO_2} \overset{K_{ads}}{\leftrightarrow} Org_{ads} \quad \text{(R4)}$$

$$Org_{ads} + TiO_2(h^+) \overset{k_{h^+}}{\rightarrow} Org^{\bullet}_{ads} + TiO_2(h^+) + H^+ \overset{Fast}{\rightarrow} P + 2H^+ \quad \text{(R5)}$$

$$2H^+ + 2TiO_2(e^-) \overset{Fast}{\rightarrow} 2H^{\bullet} \overset{Fast}{\rightarrow} H_2 \quad \text{(R6)}$$

Obviously, electron-hole pairs may recombine to produce heat and light (through reactions (7) and (8)), despite the p-n heterojunction formation boosts photogenerated charge carrier separation, resulting in better photocatalytic efficiencies with respect to those observed with bare materials.

$$TiO_2(h^+) + TiO_2(e^-) \xrightarrow{k_r} Q + light \quad (R7)$$

$$Cu_2O(h^+) + Cu_2O(e^-) \xrightarrow{k_r} Q + light \quad (R8)$$

5. Conclusions

The evaluation of the photocatalytic activity for hydrogen generation of the best-performing photocatalyst at varying organic concentrations allows the identification of an adsorption equilibrium constant of 0.22 M^{-1}. A beneficial effect is recorded with raising the system temperature, with an increase in hydrogen productivity of nearly 4.5 times with respect to the lowest temperature. Such a temperature effect is related to the higher reaction rate of hydrogen generation and the easier desorption of the products from the catalyst. As regards the effect of solution pH, alkaline conditions exert a beneficial effect on photocatalytic hydrogen generation. Under the best conditions tested (i.e., glycerol as a scavenger, pH = 12.0, T = 80 °C, and direct sunlight irradiation), a value of light-to-chemical energy efficiency of 8% in the UV range is observed. Therefore, the simple photocatalytic system is suited to visible-light-driven hydrogen generation. Despite the good performances detected under visible light irradiation only, the UV component in the solar spectrum is able to rise by 40% the photocatalytic hydrogen generation with respect to the visible light irradiation only.

Author Contributions: Conceptualization, M.M. and R.A.; methodology, M.M.; validation, L.C. and I.D.S. investigation, M.M. and M.R.; data curation, M.R. and L.C.; writing—original draft preparation, M.M., R.A. and R.M.; supervision, R.M. and R.A. All authors have read and agreed to the published version of the manuscript.

Funding: This research received no external funding.

Institutional Review Board Statement: Not applicable.

Data Availability Statement: Not applicable.

Conflicts of Interest: The authors declare no conflict of interest.

References

1. Ford, A.; Gillich, A.; Mirzania, P. Sustainable Energy and Energy Efficient Technologies. In *Future Energy*; Elsevier: Amsterdam, The Netherlands, 2020; pp. 611–630. [CrossRef]
2. Li, X.; Liu, B.; Chen, Y.; Fan, X.; Li, Y.; Zhang, F.; Zhang, G.; Peng, W. Decoration of Cu_2O photocathode with protective TiO_2 and active WS2 layers for enhanced photoelectrochemical hydrogen evolution. *Nanotechnology* **2018**, *29*, 505603. [CrossRef]
3. Hosseini, S.E.; Wahid, M.A. Hydrogen production from renewable and sustainable energy resources: Promising green energy carrier for clean development. *Renew. Sustain. Energy Rev.* **2016**, *57*, 850–866. [CrossRef]
4. Hosseini, S.E. Hydrogen from solar energy, a clean energy carrier from a sustainable source of energy. *Energy Res.* **2020**, *44*, 4110–4131. [CrossRef]
5. Møller, K.T.; Jensen, T.R.; Akiba, E. Progress in Natural Science: Materials International Hydrogen—A sustainable energy carrier. *Prog. Nat. Sci. Mater. Int.* **2017**, *27*, 34–40. [CrossRef]
6. Policastro, G.; Cesaro, A.; Fabbricino, M. Photo-fermentative hydrogen production from cheese whey: Engineering of a mixed culture process in a semi-continuous, tubular photo-bioreactor. *Int. J. Hydrogen Energy* **2022**. [CrossRef]
7. Policastro, G.; Carraturo, F.; Compagnone, M.; Guida, M.; Fabbricino, M. Enhancing hydrogen production from winery wastewater through fermentative microbial culture selection. *Bioresour. Technol. Rep.* **2022**, *19*, 101196. [CrossRef]
8. Kumaravel, V.; Mathew, S.; Bartlett, J.; Pillai, S.C. Photocatalytic hydrogen production using metal doped TiO_2: A review of recent advances. *Appl. Catal. B* **2019**, *244*, 1021–1064. [CrossRef]
9. Clarizia, L. *Hydrogen Production through Photoreforming of Oxygenated Organic Substrates over Cu/TiO$_2$* pp. 1–154. Available online: https://pdfs.semanticscholar.org/1321/7a7fd331cd35341d871297348bb274692617.pdf?_ga=2.232541020.232120235.1565266071-86349393.1556861591 (accessed on 1 January 2022).

10. Jing, D.; Guo, L.; Zhao, L.; Zhang, X.; Liu, H.; Li, M.; Shen, S.; Liu, G.; Hu, X.; Zhang, X.; et al. Efficient solar hydrogen production by photocatalytic water splitting: From fundamental study to pilot demonstration. *Int. J. Hydrogen Energy* **2010**, *35*, 7087–7097. [CrossRef]
11. Gong, J.; Li, C.J.; Wasielewski, M.R. Advances in solar energy conversion. *Chem. Soc. Rev.* **2019**, *48*, 1862–1864. [CrossRef]
12. Kar, S.K.; Sharma, A.; Roy, B. Solar energy market developments in India. *Renew. Sustain. Energy Rev.* **2016**, *62*, 121–133. [CrossRef]
13. Shaner, M.R.; Atwater, H.A.; Lewis, N.; McFarland, E.W. A comparative technoeconomic analysis of renewable hydrogen production using solar energy. *Energy Env. Sci.* **2016**, *9*, 2354–2371. [CrossRef]
14. Christoforidis, K.C.; Fornasiero, P. Photocatalytic Hydrogen Production: A Rift into the Future Energy Supply. *ChemCatChem* **2017**, *9*, 1523–1544. [CrossRef]
15. Lucchetti, R.; Onotri, L.; Clarizia, L.; di Natale, F.; di Somma, I.; Andreozzi, R.; Marotta, R. Removal of nitrate and simultaneous hydrogen generation through photocatalytic reforming of glycerol over "in situ" prepared zero-valent nano copper/P25. *Appl. Catal. B* **2017**, *202*, 539–549. [CrossRef]
16. Miwa, T.; Kaneco, S.; Katsumata, H.; Suzuki, T.; Ohta, K.; Chand Verma, S.; Sugihara, K. Photocatalytic hydrogen production from aqueous methanol solution with CuO/Al2O3/TiO2 nanocomposite. *Int. J. Hydrogen Energy* **2010**, *35*, 6554–6560. [CrossRef]
17. Yang, G.; Jiang, Z.; Shi, H.; Xiao, T.; Yan, Z. Preparation of highly visible-light active N-doped TiO_2 photocatalyst. *J. Mater. Chem.* **2010**, *20*, 5301–5309. [CrossRef]
18. Krýsa, J.; Waldner, G.; Měšťánková, H.; Jirkovský, J.; Grabner, G. Photocatalytic degradation of model organic pollutants on an immobilized particulate TiO2 layer. Roles of adsorption processes and mechanistic complexity. *Appl. Catal. B* **2006**, *64*, 290–301. [CrossRef]
19. Khoa Le, T.; Flahaut, D.; Martinez, H.; Hung Nguyen, H.K.; Xuan Huynh, T.K. Huynh Study of the effects of surface modification by thermal shock method on photocatalytic activity of TiO2 P25. *Appl. Catal. B* **2015**, *165*, 260–268. [CrossRef]
20. Al-Azri, Z.H.N.; Chen, W.T.; Chan, A.; Jovic, V.; Ina, T.; Idriss, H.; Waterhouse, G.I.N. The roles of metal co-catalysts and reaction media in photocatalytic hydrogen production: Performance evaluation of M/TiO_2 photocatalysts (M = Pd, Pt, Au) in different alcohol-water mixtures. *J. Catal.* **2015**, *329*, 355–367. [CrossRef]
21. Chen, X.; Shen, S.; Guo, L.; Mao, S.S. Semiconductor-based photocatalytic hydrogen generation. *Chem. Rev.* **2010**, *110*, 6503–6570. [CrossRef]
22. Wang, X.; Dong, H.; Hu, Z.; Qi, Z.; Li, L. Fabrication of a Cu2O/Au/TiO2composite film for efficient photocatalytic hydrogen production from aqueous solution of methanol and glucose. *Mater. Sci. Eng. B. Solid State Mater. Adv. Technol.* **2017**, *219*, 10–19. [CrossRef]
23. Zhang, X.; Peng, T.; Song, T. Recent advances in dye-sensitized semiconductor systems for photocatalytic hydrogen production. *J. Mater. Chem. A Mater.* **2016**, *4*, 2365–2402. [CrossRef]
24. Jones, W.; Martin, D.J.; Caravaca, A.; Beale, A.M.; Bowker, M.; Maschmeyer, T.; Hartley, G.; Masters, A. A comparison of photocatalytic reforming reactions of methanol and triethanolamine with Pd supported on titania and graphitic carbon nitride. *Appl. Catal. B* **2019**, *240*, 373–379. [CrossRef]
25. Singh, R.; Dutta, S. A review on H2 production through photocatalytic reactions using TiO_2/TiO_2-assisted catalysts. *Fuel* **2018**, *220*, 607–620. [CrossRef]
26. Ismail, A.A.; Al-sayari, S.A.; Bahnemann, D.W. Photodeposition of precious metals onto mesoporous TiO_2 nanocrystals with enhanced their photocatalytic activity for methanol oxidation. *Catal. Today* **2013**, *209*, 2–7. [CrossRef]
27. Basavarajappa, P.S.; Patil, S.B.; Ganganagappa, N.; Reddy, K.R.; Raghu, A.v.; Reddy, C.V. Recent progress in metal-doped TiO_2, non-metal doped/codoped TiO_2 and TiO_2 nanostructured hybrids for enhanced photocatalysis. *Int. J. Hydrogen Energy* **2020**, *45*, 7764–7778. [CrossRef]
28. Clarizia, L.; Russo, D.; di Somma, I.; Andreozzi, R.; Marotta, R. *Metal-Based Semiconductor Nanomaterials for Photocatalysis*; Elsevier Ltd.: Amsterdam, The Netherlands, 2018. [CrossRef]
29. Bazzo, A.; Urakawa, A. Understanding synergetic effects of Zn and Rh–Cr promotion to wide-bandgap Ga, Ta and Ti oxides in photocatalytic water splitting. *Catal. Sci. Technol.* **2016**, *6*, 4243–4253. Available online: https://www.bing.com/search?q=A.+Bazzo%2C+A.+Urakawa%2C+Understanding+synergetic+effects+of+Zn+and+Rh%E2%80%93Cr+promotion+to+wide-bandgap+Ga%2C+Ta+and+Ti+oxides+in+photocatalytic+water+splitting%2C+Catal.+Sci.+Technol.+6+%282016%29+4243%E2%80%934253.&form=ANNH01&refig=813e43e752ea4ac4ac74e87e30375be2 (accessed on 13 September 2021). [CrossRef]
30. Humayun, M.; Raziq, F.; Khan, A.; Luo, W. Modification strategies of TiO_2 for potential applications in photocatalysis: A critical review. *Green Chem. Lett. Rev.* **2018**, *11*, 86–102. [CrossRef]
31. Muscetta, M.; Russo, D. Photocatalytic applications in wastewater and air treatment: A patent review (2010–2020). *Catalysts* **2021**, *11*, 834. [CrossRef]
32. Sakthivel, S.; Geissen, S.U.; Bahnemann, D.W.; Murugesan, V. Vogelpohl, A. Enhancement of photocatalytic activity by semiconductor heterojunctions: α-Fe_2O_3, WO3 and CdS deposited on ZnO. *J. Photochem. Photobiol. A Chem.* **2002**, *148*, 283–293. [CrossRef]
33. Jeong, S.S.; Mittiga, A.; Salza, E.; Masci, A. Passerini, S. Electrodeposited ZnO/Cu_2O heterojunction solar cells. *Electrochim. Acta.* **2008**, *53*, 2226–2231. [CrossRef]
34. Bessekhouad, Y.; Robert, D.; Weber, J.v. Photocatalytic activity of Cu_2O/TiO_2, Bi_2O_3/TiO_2 and $ZnMn_2O_4$/TiO_2 heterojunctions. *Catal. Today* **2005**, *101*, 315–321. [CrossRef]

35. Lv, P.; Lin, L.; Zheng, W.; Zheng, M.; Lai, F. Photosensitivity of ZnO/Cu_2O thin film heterojunction. *Optik* **2013**, *124*, 2654–2657. [CrossRef]
36. Reza Gholipour, M.; Dinh, C.T.; Béland, F.; Do, T.O. Nanocomposite heterojunctions as sunlight-driven photocatalysts for hydrogen production from water splitting. *Nanoscale* **2015**, *7*, 8187–8208. [CrossRef]
37. Wang, H.; Zhang, L.; Chen, Z.; Hu, J.; Li, S.; Wang, Z.; Liu, J.; Wang, X. Semiconductor heterojunction photocatalysts: Design, construction, and photocatalytic performances. *Chem. Soc. Rev.* **2014**, *43*, 5234–5244. [CrossRef]
38. Niu, W.; Moehl, T.; Cui, W.; Wick-Joliat, R.; Zhu, L.; Tilley, S.D. Extended Light Harvesting with Dual Cu2O-Based Photocathodes for High Efficiency Water Splitting. *Adv. Energy Mater.* **2018**, *8*, 1702323. [CrossRef]
39. Yan, L.; Yang, F.; Tao, C.Y.; Luo, X.; Zhang, L. Highly efficient and stable Cu_2O–TiO_2 intermediate photocatalytic water splitting. *Ceram. Int.* **2020**, *46*, 9455–9463. [CrossRef]
40. Le, L.; Wu, Y.; Zhou, Z.; Wang, H.; Xiong, R.; Shi, J. Cu_2O clusters decorated on flower-like TiO_2 nanorod array film for enhanced hydrogen production under solar light irradiation. *J. Photochem. Photobiol. A Chem.* **2018**, *351*, 78–86. [CrossRef]
41. Muscetta, M.; Andreozzi, R.; Clarizia, L.; di Somma, I.; Marotta, R. Hydrogen production through photoreforming processes over Cu_2O/TiO_2 composite materials: A mini-review. *Int. J. Hydrogen Energy* **2020**, *45*, 28531–28552. [CrossRef]
42. Muscetta, M.; al Jitan, S.; Palmisano, G.; Andreozzi, R.; Marotta, R.; Cimino, S.; di Somma, I. Visible light—driven photocatalytic hydrogen production using Cu_2O/TiO_2 composites prepared by facile mechanochemical synthesis. *J. Environ. Chem. Eng.* **2022**, *10*, 107735. [CrossRef]
43. Cheng, P.; Li, W.; Zhou, T.; Jin, Y.; Gu, M. Physical and photocatalytic properties of zinc ferrite doped titania under visible light irradiation. *J. Photochem. Photobiol. A Chem.* **2004**, *168*, 97–101. [CrossRef]
44. Muscetta, M.; Clarizia, L.; Garlisi, C.; Palmisano, G.; Marotta, R.; Andreozzi, R.; Ii, F.; Chimica, I.; Industriale, P. Hydrogen production upon UV-light irradiation of Cu/TiO 2 photocatalyst in the presence of alkanol- amines. *Int. J. Hydrogen Energy* **2020**, *45*, 26701–26715. [CrossRef]
45. Clarizia, L.; Di Somma, I.; Onotri, L.; Andreozzi, R.; Marotta, R. Kinetic modeling of hydrogen generation over nano-Cu(s)/TiO_2 catalyst through photoreforming of alcohols. *Catal. Today* **2017**, *281*, 117–123. [CrossRef]
46. Badawy, M.I.; Ghaly, M.Y.; Ali, M.E.M. Photocatalytic hydrogen production over nanostructured mesoporous titania from olive mill wastewater. *Desalination* **2011**, *267*, 250–255. [CrossRef]
47. Lin, W.C.; Yang, W.D.; Huang, I.L.; Wu, T.S.; Chung, Z.J. Hydrogen production from methanol/water photocatalytic decomposition using pt/tio2-xnx catalyst. *Energy Fuels* **2009**, *23*, 2192–2196. [CrossRef]
48. El-Bindary, M.A.; El-Desouky, M.G.; El-Bindary, A.A. Metal–organic frameworks encapsulated with an anticancer compound as drug delivery system: Synthesis, characterization, antioxidant, anticancer, antibacterial, and molecular docking investigation. *Appl. Organomet. Chem.* **2022**, *36*, e6660. [CrossRef]
49. Wu, Y.; Lu, G.; Li, S. The role of Cu(I) species for photocatalytic hydrogen generation over CuOx/TiO_2. *Catal. Lett.* **2009**, *133*, 97–105. [CrossRef]
50. Karimi Estahbanati, M.R.; Mahinpey, N.; Feilizadeh, M.; Attar, F.; Iliuta, M.C. Kinetic study of the effects of pH on the photocatalytic hydrogen production from alcohols. *Int. J. Hydrogen Energy* **2019**, *44*, 32030–32041. [CrossRef]
51. Corredor, J.; Rivero, M.J.; Rangel, C.M.; Gloaguen, F.; Ortiz, I. Comprehensive review and future perspectives on the photocatalytic hydrogen production. *J. Chem. Technol. Biotechnol.* **2019**, *94*, 3049–3063. [CrossRef]
52. Clarizia, L.; Spasiano, D.; di Somma, I.; Marotta, R.; Andreozzi, R.; Dionysiou, D.D. Copper modified-TiO_2 catalysts for hydrogen generation through photoreforming of organics. A short review. *Int J Hydrogen Energy* **2014**, *39*, 16812–16831. [CrossRef]
53. Xu, S.; Ng, J.; Zhang, X.; Bai, H.; Sun, D.D. Fabrication and comparison of highly efficient Cu incorporated TiO_2 photocatalyst for hydrogen generation from water. *Int J Hydrog. Energy* **2010**, *35*, 5254–5261. [CrossRef]
54. Serjeant, E.P.; Dempsey, B. *Ionisation Constants of Organic Acids in Aqueous Solution*; Pergamon Press: Oxford, UK, 1979.
55. Kosmulski, M. Isoelectric points and points of zero charge of metal (hydr)oxides: 50 years after Parks' review. *Adv. Colloid. Interface Sci.* **2016**, *238*, 1–61. [CrossRef] [PubMed]
56. Hu, J.; Wang, J.; Liu, S.; Zhang, Z.; Zhang, H.; Cai, X.; Pan, J.; Liu, J. Effect of TiO_2 nanoparticle aggregation on marine microalgae Isochrysis galbana. *J. Environ. Sci.* **2018**, *66*, 208–215. [CrossRef]
57. Gao, M.; Zhang, T.; Ho, G.W. Advances of photothermal chemistry in photocatalysis, thermocatalysis, and synergetic photothermocatalysis for solar-to-fuel generation. *Nano Res.* **2022**, *15*, 9985–10005. [CrossRef]
58. Reza, M.S.; Ahmad, N.B.H.; Afroze, S.; Taweekun, J.; Sharifpur, M.; Azad, A.K. Hydrogen Production from Water Splitting through Photocatalytic Activity of Carbon-Based Materials. *Chem. Eng. Technol.* **2022**. [CrossRef]
59. Huaxu, L.; Fuqiang, W.; Ziming, C.; Shengpeng, H.; Bing, X.; Xiangtao, G.; bo, L.; Jianyu, T.; Xiangzheng, L.; Ruiyang, C.; et al. Analyzing the effects of reaction temperature on photo-thermo chemical synergetic catalytic water splitting under full-spectrum solar irradiation: An experimental and thermodynamic investigation. *Int. J. Hydrogen Energy* **2017**, *42*, 12133–12142. [CrossRef]
60. Zhang, Z.; Maggard, P.A. Investigation of photocatalytically-active hydrated forms of amorphous titania, $TiO_2 \cdot nH_2O$. *J. Photochem. Photobiol. A Chem.* **2007**, *186*, 8–13. [CrossRef]
61. Song, R.; Luo, B.; Geng, J.; Song, D.; Jing, D. Photothermocatalytic Hydrogen Evolution over Ni2P/TiO2 for Full-Spectrum Solar Energy Conversion. *Ind. Eng. Chem. Res.* **2018**, *57*, 7846–7854. [CrossRef]
62. Velázquez, J.J.; Fernández-González, R.; Díaz, L.; Pulido Melián, E.; Rodríguez, V.D.; Núñez, P. Effect of reaction temperature and sacrificial agent on the photocatalytic H2-production of Pt-TiO_2. *J. Alloy. Compd.* **2017**, *721*, 405–410. [CrossRef]

63. Rico-Oller, B.; Boudjemaa, A.; Bahruji, H.; Kebir, M.; Prashar, S.; Bachari, K.; Fajardo, M.; Gómez-Ruiz, S. Photodegradation of organic pollutants in water and green hydrogen production via methanol photoreforming of doped titanium oxide nanoparticles. *Sci. Total Environ.* **2016**, *563–564*, 921–932. [CrossRef]
64. Munusamy, T.D.; Chin, S.Y.; Tarek, M.; Khan, M.M.R. Sustainable hydrogen production by CdO/exfoliated g-C3N4 via photoreforming of formaldehyde containing wastewater. *Int. J. Hydrogen Energy* **2021**, *46*, 30988–30999. [CrossRef]
65. Koca, A.; Ahin, M.S. Photocatalytic Hydrogen Production by Direct Sun Light from Sulfide=Sulfite Solution. 2002. Available online: www.elsevier.com/locate/ijhydene (accessed on 1 January 2022).
66. Wei, Z.; Liu, J. Shangguan, W. A review on photocatalysis in antibiotic wastewater: Pollutant degradation and hydrogen production. *Chin. J. Catal.* **2020**, *41*, 1440–1450. [CrossRef]
67. Chowdhury, P.; Malekshoar, G.; Ray, M.B.; Zhu, J.; Ray, A.K. Sacrificial hydrogen generation from formaldehyde with Pt/TiO_2 photocatalyst in solar radiation. *Ind. Eng. Chem. Res.* **2013**, *52*, 5023–5029. [CrossRef]
68. Zhang, S.; Wang, L.; Liu, C.; Luo, J.; Crittenden, J.; Liu, X.; Cai, T.; Yuan, J.; Pei, Y.; Liu, Y. Photocatalytic wastewater purification with simultaneous hydrogen production using MoS2 QD-decorated hierarchical assembly of ZnIn2S4 on reduced graphene oxide photocatalyst. *Water Res.* **2017**, *121*, 11–19. [CrossRef] [PubMed]
69. Riddick, J.A.; Bunger, W.B.; Sakano, T.K. *Organic Solvents: Physical Properties and Methods of Purification*, 4th ed.; Wiley-Interscience: New York, NY, USA, 1986.
70. Williams, M. *The Merck Index: An Encyclopedia of Chemicals, Drugs, and Biologicals*, 15th ed.; Royal Society of Chemistry: Cambridge, UK, 2013.

Disclaimer/Publisher's Note: The statements, opinions and data contained in all publications are solely those of the individual author(s) and contributor(s) and not of MDPI and/or the editor(s). MDPI and/or the editor(s) disclaim responsibility for any injury to people or property resulting from any ideas, methods, instructions or products referred to in the content.